MATEC Web of Conferences **413**, 01002 (2025) https://doi.org/10.1051/matecconf/202541301002
MAIQS 2025

Self-calibration measurement and uncertainty evaluation of lens focal length based on Fabry-Perot Interferometer

Zelin Li[1], *Xiaoyan* Shen[1*], *Lei* Li[1], and *Wenxia* Kong[1]

[1] College of Metrology Measurement and Instrument, China Jiliang University, Hangzhou, Zhejiang 310018, China

Abstract: This paper proposes a self-calibration method for lens focal length measurement based on a Fabry-Pérot (F-P) etalon, and investigates uncertainty evaluation strategies in scenarios where measurement errors affect the results through indirect propagation. In the measurement method, the relationship between the diameters of interference rings and interference orders in area-array images is utilized, and the relative focal length is calculated using the least squares method. For uncertainty analysis, evaluation models suitable for both the Guide to the Expression of Uncertainty in Measurement (GUM) method and the Monte Carlo method (MCM) are established. In the Monte Carlo method, error propagation approaches are specifically studied for defocus error and pixel pitch error in focal length measurement. The results show that the GUM evaluation method fails to pass validation by MCM, mainly because the distribution of the relative focal length deviates from the t-distribution assumption. Furthermore, this study proposes an uncertainty evaluation process applicable to such indirect measurement models, which provides a valuable reference for complex optical measurement systems.

Key words: Focal length measurement; Error propagation; Monte Carlo method; Uncertainty analysis.

1 Introduction

Focal length is one of the key parameters of an optical system. Common methods for measuring focal length include the collimated beam focusing method, the secondary imaging method, and the autocollimation method, among others. However, as the demand for higher precision in focal length measurement increases, the accuracy of conventional methods is no longer sufficient, prompting the development of more advanced techniques. Du et al. [1] proposed a high-precision laser differential confocal method for focal length measurement based on eccentricity suppression. When measuring a lens with a 100 mm focal length, this method achieved a relative repeatability (RMS) of 0.000503%. Li [2] measured the focal length of a thin convex lens using a collimator method, achieving a relative error of only 0.138% for a nominal 100 mm lens. Fei Xianxiang et al. [3] used an object-image parallax comparison method to measure the focal length of a 225 mm lens, yielding a relative deviation of 0.13%. He et al. [4] proposed a method based on correlation coefficient matching to measure the focal lengths of convex and concave lenses. For a biconvex lens with a focal length of 175.578 mm and a biconcave lens with a focal length of −100.001 mm, the relative measurement errors were 0.126% and 0.202%, respectively. Cao et al. [5] introduced a method using a diffractive beam sampler to measure lens focal lengths. Their experiments with lenses ranging from 25 mm to 100 mm in focal length demonstrated relative errors of less than 0.1%. Dou et al. [6] proposed a method based on vortex beam interference for measuring the focal lengths of convex and concave lenses, achieving relative errors of 0.0892% for a 200 mm biconvex lens and a −100 mm biconcave lens. However, these studies generally lack sufficient attention to measurement uncertainty, even though a proper evaluation of uncertainty is crucial for correctly interpreting measurement results.

Currently, there are two commonly used methods for uncertainty evaluation: The Guide to the Expression of Uncertainty in Measurement (GUM) and the Monte Carlo Method (MCM). GUM relies more heavily on mathematical analysis, while MCM depends on simulation [7]. The Joint Committee for Guides in Metrology (JCGM) recommends using both GUM and MCM to evaluate uncertainty and compare results. Compared with GUM, MCM is more universally applicable to various models and distributions, offering greater practicality, richer output information [8], and

*Corresponding author: xyshen@cjlu.edu.cn

reduced analytical effort for complex or nonlinear models [9].

In earlier work, our research group studied a method for focal length measurement based on Fabry-Pérot (F-P) etalons. We developed a technique that determines focal length by processing interference rings captured by an area array sensor. To improve measurement accuracy, GUM- and MCM-based uncertainty evaluation models were established according to the principles of focal length measurement. The focal length measurement apparatus was optimized, and a Monte Carlo-based uncertainty evaluation method was proposed for cases involving error propagation. A comparative analysis of both methods was conducted to provide a reliable basis for interpreting the evaluation results.

2 Principle of self-calibrated focal length measurement and uncertainty analysis

2.1 Principle of focal length measurement

As shown in Figure 1, the light source first passes through a filter to produce monochromatic light with a wavelength of λ_0. This light then passes through a Fabry-Pérot (F-P) etalon with a spacing of d and an air gap refractive index of n, generating a series of conical beams. After passing through the test transmission objective lens with a focal length f, the conical beams form a series of concentric interference rings with diameters D_i on the area array image sensor. Here, i denotes the index of the interference ring, starting from the center. When i=0,1,2…, the integer parts of the corresponding interference orders are k_i=k_0,k_0-1,…,k_0-i, where k_0 is the integer part of the interference order corresponding to the smallest emission angle θ_i(i=0).The corresponding integer interference order is given by $2dn/\lambda_0=k_0+\varepsilon$, where ε is the fractional part of this order.

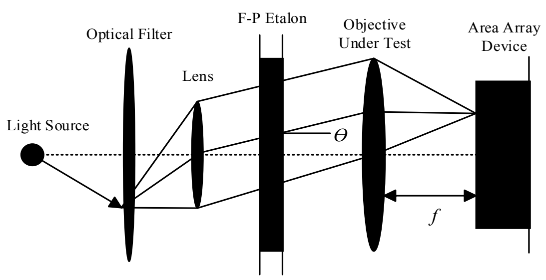

Fig.1 principle of focal length measurement for transmission objective lenses

To facilitate calculation, the diameters of the concentric rings $D_{i,w}$ and the focal length f_w are both expressed in relative units based on the average pixel pitch w of the area array sensor. The relationship among the concentric ring diameter $D_{i,w}$, the interference angle θ_i, and the normalized focal length f_w is as follows [10]:

$$(\frac{D_{i,w}/2}{f_w})^2 = (\tan\theta_i)^2 = (\frac{k_0+\varepsilon}{k_0-\varepsilon})^2 - 1 \tag{1}$$

From Equation (1), it can be seen that there exists a one-to-one correspondence between the concentric ring diameter $D_{i,w}$ and the ring order i. Based on this relationship, the fractional part of the interference order, ε, can be determined, which can then be used to further calculate the normalized focal length f_w.

By rearranging Equation (1), the simplified form of the equation is obtained as follows:

$$-i \approx \widetilde{\varepsilon} - \frac{k_0}{8(f_w)^2} D_{i,w}{}^2 \tag{2}$$

In the formula, $\widetilde{\varepsilon}$ is the approximate value of ε. According to Equation (2), when different ring serial numbers i and the corresponding $D_{i,w}$ are obtained, the intercept $\widetilde{\varepsilon}$ can be calculated using the method of least squares fitting.

Retransform Equation (1), retain terms up to the second order of small quantities, and rearrange to obtain:

$$D_i^2 = b_0 + b_1 i^* = \frac{8(f_w)^2}{k_0}\varepsilon(1+\frac{\varepsilon}{2k_0}) + \frac{8(f_w)^2}{k_0} i^* \tag{3}$$

$$i^* = (1 + (1.5i + 2\widetilde{\varepsilon})/k_0)i \tag{4}$$

From Equations (3) and (4), it can be seen that the slope b_1 and the standard deviation S_{b1} can be obtained through linear fitting. From Equations (3), the relative focal length and its relative standard deviation can be obtained as:

$$f_w = \sqrt{b_1 k_0 / 8} \tag{5}$$

$$\frac{s_{f_w}}{f_w} = \frac{s_{b_1}}{2b_1} \tag{6}$$

From Equation (5), the focal length f is:

$$f = w \cdot (f_w) \tag{7}$$

2.2 Analysis of the focal length self-calibration measurement results

From Equation (5), it is evident that the accuracy of the focal length measurement is directly related to the integer part of the interference order k_0. According to the formula for $2dn/\lambda_0=k_0+\varepsilon$, k_0 can be expressed as:

$$k_0 = \mathrm{int}(\frac{2nd}{\lambda_0}) \tag{8}$$

where int denotes the floor function. Observing Equation (8), it is evident that the primary factors influencing the accuracy of the integer part of the interference order k_0 are the refractive index of air n and the spacing d of the Fabry-Pérot (F-P) etalon. The U.S. National Institute of Standards and Technology (NIST) provides values for vacuum wavelengths with standard uncertainties that can reach a level of 10^{-8}. Based on this, by performing controlled measurements of local air temperature and pressure, an air refractive index with comparable accuracy can be obtained [11]. Therefore, the key parameter limiting the accuracy of k_0 is the F-P spacing d.

According to the classical and traceable geometric measurement method, that is multi-wavelength fractional-order method, discussed by Born M. and Wolf E., the F-P etalon spacing d can be measured precisely.

This approach also enables d to be traced back to standard spectral line wavelengths. Once d is accurately determined, the k_0 corresponding to the center of the concentric interference rings captured by the area array sensor can be accurately obtained. This, in turn, enables precise measurement of the focal length f, thus achieving self-calibrated focal length measurement.

2.3 Principle of measuring the spacing *d* of the F-P standard by the fractional reversing method

The spacing d of the F-P standard can generally be expressed as:

$$d=\frac{1}{2}\lambda_j(k_{0j}+\varepsilon_j)=\frac{\lambda_{0j}}{2n}(k_{0j}+\varepsilon_j) \tag{9}$$

where j=1,2,3, k_{0j} represents the integer part of the first ring interference order from the inside out, and ε_j represents the corresponding fractional part. Using three monochromatic lights of wavelengths λ_j the fractional parts of the corresponding interference orders can be measured accurately. Based on the system of equations:

$$d=0.5\lambda_j(k_{0j}+\varepsilon_j) \tag{10}$$

The spacing d of the Fabry-Pérot etalon can be accurately determined. The fractional part ε_j is solved according to Equation (3). After solving for the corresponding intercept b_{0j} and slope b_{1j},the following can be obtained:

$$\varepsilon_j=\frac{-b_{0j}}{b_{1j}}\left[1+1.5\frac{(-b_{0j}/b_{1j})}{k_{0j}}\right] \tag{11}$$

Due to the expansion uncertainty $U_{\varepsilon j}$ of the fractional part affecting the solution, too small an uncertainty can lead to no solution, while too much can lead to multiple solutions. Therefore, it is necessary to seek the uncertainty of the fractional part. Based on the research by Liu [12], Lan [13], and others, the standard deviation ε_j of the fractional part S_{ε_j} ,Type A uncertainty $u_{\varepsilon,A}$,Type B uncertainty $u_{\varepsilon,B}$ and the calculation formula for the combined uncertainty $u_{\varepsilon j}$ are:

$$\begin{aligned}\frac{s_{\varepsilon_j}}{\varepsilon_j}&\approx\frac{s_{b_{0j}/b_{1j}}}{-b_{0j}/b_{1j}}\\&=\sqrt{(\frac{s_{b_{0j}}}{b_{0j}})^2+(\frac{s_{b_{1j}}}{b_{1j}})^2-2r_{b_{1j},b_{0j}}(\frac{s_{b_{0j}}}{b_{0j}})(\frac{s_{b_{1j}}}{b_{1j}})}\end{aligned} \tag{12}$$

$$u_{\varepsilon,A}=\sqrt{s_\varepsilon^2+(\frac{\sqrt{3}s_{D_i^2}}{2b_1})^2} \tag{13}$$

$$u_{\varepsilon,B}\approx(\frac{u_{D_{i,j}^2,B}}{-b_{1,j}})\frac{\varepsilon_j-\bar{i}_j}{i_{\max}-\bar{i}_j} \tag{14}$$

In the formula, $s_{b_{0j}}$ is the combined standard uncertainty of the intercept,$s_{b_{1j}}$is the combined standard uncertainty of the slope, $s_{D_i^2}$is the combined standard uncertainty of the diameter,$\bar{\imath}_j$ is the average value of the measured orders for each wavelength. $u_{D_{ij}^2,B}$ can be calculated using Equation (15):

$$u_{D_{i,j}^2,B}=\frac{-0.1b_{1j}}{F} \tag{15}$$

where F is the estimated fineness of the F-P standard. The ratio of the radius difference between adjacent rings to the radius of the ring half-height width F_w in the F-P interference imaging ring is used. The calculation method is as follows:

$$F\approx\frac{R_{k-1}-R_k}{F_w} \tag{16}$$

Combine s_ε with $u_{\varepsilon,B}/\sqrt{3}$ and based on the t-distribution formula, calculate the effective degrees of freedom v_{eff} ,With p=0.95,the combined standard uncertainty is obtained as:

$$u_{\varepsilon j}=t(v_{eff})\sqrt{(s_{\varepsilon,A})^2+(u_{\varepsilon,B}/\sqrt{3})^2} \tag{17}$$

Through the above calculations, the known quantities obtained are: the estimated spacing d_0 of the F-P standard and three sets (λ_j,ε_j,u_ε). First, find the maximum vacuum wavelength $u_{\varepsilon,j}$ of λ_{j1}.From the estimated spacing d_0 of the F-P standard, the integer order estimate k_{01} is determined by k_{01}=int（$2d_0/\lambda_{a1}$）, where λ_{a1}=λ_{a1}/n. Then, determine the central values of 200 intervals with λ_{a1}.

$$d_1=(k_{01}+\varepsilon_1+l)\lambda_{a1}/2 \tag{18}$$

where l=±1,±2,⋯,±100.

Next, mark 1000 equidistant points within the interval $(d_1+u_{\varepsilon 1})\lambda_{a1}/2$ for each d_2:

$$d_2=(k_{01}+\varepsilon_1+l+m/500)\lambda_{a1}/2 \tag{19}$$

where m=±1,±2,⋯,±500.

Then, for each point d_2 within each interval, calculate the fractional parts $\varepsilon_{l2},\varepsilon_{l3}$,corresponding to the remaining two wavelengths to satisfy Equation (20):

$$\begin{cases}|\varepsilon_{l2}-\varepsilon_2|\le u_{\varepsilon 2}\\|\varepsilon_{l3}-\varepsilon_3|\le u_{\varepsilon 3}\end{cases} \tag{20}$$

Identify all the continuous points that satisfy Equation (20), calculate the average value $\overline{d_1}$ of these continuous points within each interval, and the range half-widthΔd. Observe the results; when $\overline{d_1}$ has only one solution, the F-P standard spacing d can be clearly obtained. If there are multiple solutions, based on $\overline{d_1}$ and the three wavelengths, calculate the average root of the relative deviation of the fractional parts from the original fractional parts, and judge the reasonableness of the value based on its magnitude.

2.4 Error sources and propagation mechanism analysis

According to the principle of focal length calculation, the primary sources of uncertainty in focal length measurement include U_1: the component caused by defocusing of the area array sensor, U_2: the uncertainty due to the standard deviation in linear fitting, U_3: the uncertainty introduced by temperature variations.

Uncertainty Component U_1 caused by defocusing of the area array sensor. The imaging situation of the array device located behind the ideal focal plane is shown in Figure 2.

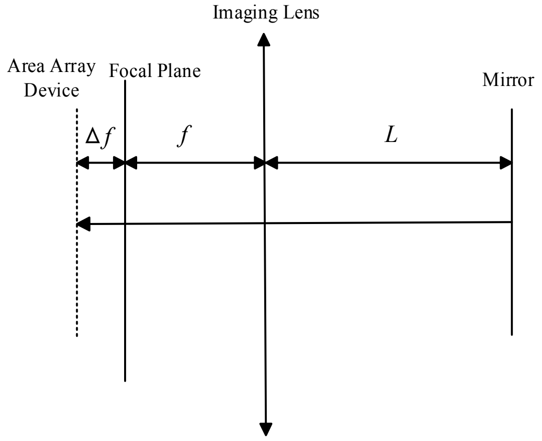

Fig.2 schematic of defocus for area array device

In Figure 2, L represents the linear distance between the optical center of the imaging lens and the mirror, while f denotes the defocus amount of the area array sensor. The presence of defocus error introduces inaccuracies in the determination of ring diameters, which in turn leads to errors in focal length measurement. In the experiment, the focusing error was estimated using a defined focusing error limit to account for this source of uncertainty.

The defocus error limit $U_{f_{ad}}$ represents the allowable error range of the distance that the array device deviates from the ideal focal plane during the focusing process, which is mainly calculated based on the half-height width F_w and the standard deviation s_{f_w} of the half-height width. First, according to the light intensity distribution of the image, a certain function is used, and based on the weighted multiple regression, the half-height width F_w and its standard deviation s_{f_w} are obtained [14].

The uncertainty U_2 due to linear fitting standard deviations elect a certain number of rings, combine with Equation (2), and use the method of linear fitting to find the intercept $\tilde{\varepsilon}$, and use $\tilde{\varepsilon}$ to obtain i^*. Calculate k_0 using $2dn/\lambda_0 = k_0 + \varepsilon$ .Based on the parameters already obtained, solve Equation (3) by fitting to find the slope $b_1$and intercept f_w. According to Equation (6), obtain the relative standard deviation of f_w.

The uncertainty U_3 caused by temperature variations. In this study, the pixel pitch w is used as the unit for focal length measurement. However, temperature variations can cause a deviation between the actual and theoretical values of w. The calibration of w is typically carried out by one-dimensional translation measurement systems that are free from Abbe error, such as laser interferometers. According to reference [10], the influence of temperature on the pixel pitch—and consequently on focal length measurement—is negligible. Therefore, in practical experiments, the measurement error in focal length due to temperature variation is not considered.

Based on the above analysis of uncertainty sources and according to Equation (7), the relative expanded uncertainty of the focal length f is expressed as:

$$\frac{U_f}{f} = t_v \cdot \sqrt{\left(\frac{S_{f_w}}{f_w}\right)^2 + \left(\frac{U_{f_{ad}}}{2f}\right)^2 + \left(\frac{U_w}{\sqrt{3}w}\right)^2} \tag{21}$$

where t_v is the expansion factor under the degree of freedom t_{eff} and the degree of freedom t_{eff} is based on the t-distribution formula, which is specifically determined according to the experiment; $U_{f_{ad}}$ is the uncertainty component brought by the defocus error; S_{f_w} is the relative standard deviation of the focal distance obtained in the linear fitting process. U_w is the expansion uncertainty of the average pixel distance.

3 Measurement and evaluation based on the GUM method

3.1 Measurement apparatus

A measurement setup was designed as shown in Figure 3 to collect and process relevant data. A mercury lamp was placed in front of the filtering device, which consists of a dual-aperture sliding insert and two sets of optical filters. The light passes through a converging lens and the F-P etalon to form a conical beam. This beam is then reflected by a mirror, passes through the test fixed-focus lens, and finally forms an image on an industrial camera, where it is captured for further analysis.

The F-P etalon used has a reflectance of 90%. The industrial camera is a HIKVISION MV-CH430-90XM with a pixel size of 2.8 μm. The fixed-focus lens used is a HIKVISION MVL-LF8040M-F, with a nominal focal length of 80 mm.

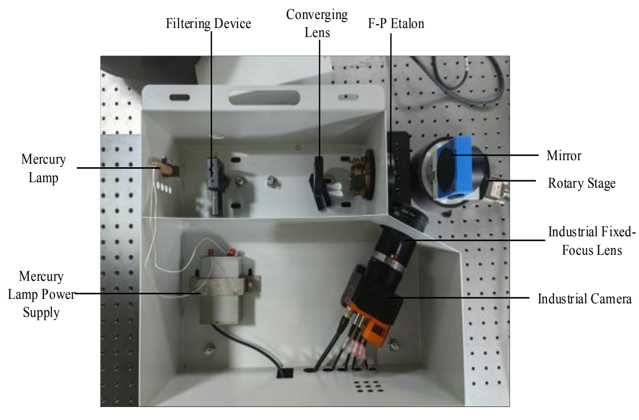

Fig.3 focal length measurement device

3.2 Measuring the spacing *d* of the F-P standard by the fractional reversing method

Based on the measurement principle described in Section 2.3, calculations were performed using three wavelengths: 546 nm, 576 nm, and 579 nm. The 576 nm and 579 nm wavelengths were generated using a yellow optical filter, resulting in dual-line concentric interference rings on the area array sensor, as shown in Figure 4.

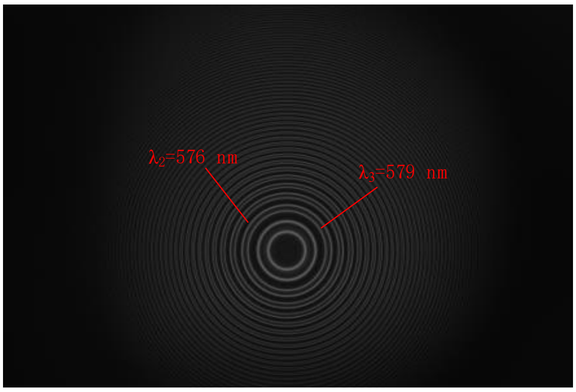

Fig.4 two-line interferometric torus image

According to the principle of fractional order combination measurement for determining the F-P etalon spacing described in Section 2.3, the final calculated F-P etalon spacing is:d=(2009.96658±0.00006)μm.

3.3 Modeling and measurement of defocus error

The lens focusing ring was set to its initial position. By rotating the focusing ring, the position of the image plane was adjusted so that the interference ring images captured by the camera underwent a transition from defocused to relatively sharp and then back to defocused. When the focusing ring was rotated by a known step size, the object-image distance changed in a controlled manner, thereby introducing a defocus displacement of a known magnitude. By acquiring images at each step position, the maximum allowable deviation of the area array device from the focal plane could be calculated. The focusing ring was rotated in steps of 50μm, and a series of images, as shown in Figure 5, were collected. The F_w value of the 10th ring in each image was then determined.

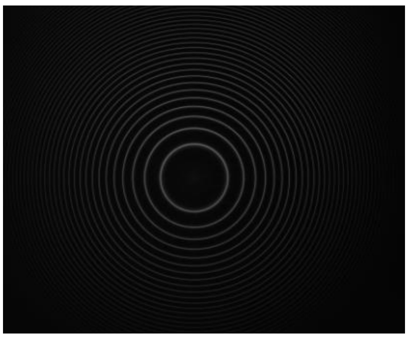

Fig.5 interference rings collected

Fit the obtained set of $F_w(x)$ values according to Equation (22) to derive the functional model shown in Figure 6.

$$F_w(x) = a_0 + a_1 x + a_2 x^2 + a_3 x^4 \tag{22}$$

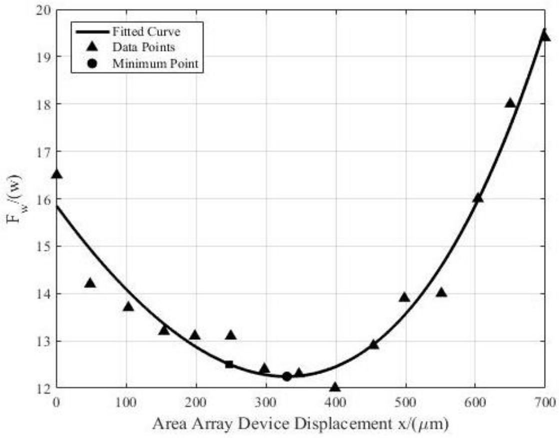

Fig.6 fitted curve with a step size of 50 μm

Based on the fitted function model, the corresponding minimum full width at half maximum $F_{w_{\min}}$ and its standard deviation s_{f_w} can be determined. The focus ring is then adjusted to the corresponding position $(F_{w_{\min}}+2s_{F_w})$, and an image is captured.

The full width at half maximum of this image is substituted into the fitted function $F_w(x)$,yielding two solutions x_1 and x_2,the half-width of the interval defined by these two solutions is taken as the focusing error limit $U_{f_{ad}}$,and the final calculated result is $U_{f_{ad}}$=79.5μm.

3.4 Analysis and calculation of linear fitting error

A total of 12 ring diameters corresponding to i = 0, 1, 2, ..., 11 are selected for analysis. First, a linear fitting is performed based on Equation(2) to derive the intercept $\tilde{\varepsilon}$,which represents the estimated value of ε. Next, using the obtained ε value, Equation(4) is applied to calculate i^*, while the slope b_1 in Equation(3) is determined through fitting. The squared diameter values for rings with different indices and their corresponding calculated i^* values are presented in Table 1.

Tab.1 The values of D_i^2 for different ring serial numbers and i^*

i	D_i^2/w	i^*
0	523877.23	0
1	950273.09	1.000
2	1376494.57	2.001
3	1802925.39	3.002
4	2229473.04	4.004
5	2656125.91	5.006
6	3082847.81	6.009
7	3509679.58	7.012
8	3936591.54	8.015
9	4363768.20	9.019
10	4790894.70	10.023
11	5218292.80	11.028

The parameter k_0=7361 was calculated from $2dn/\lambda_0=k_0+\varepsilon$.Based on Equation(3), fitting yielded a slope b_1=425663.986588050,with f_w=19790.25,and the degree of freedom v=10.The relative standard deviation $s_{b_1}/2b_1$=0.000037 for the relative focal length was then derived using Equation (22).

3.5 Experimental data analysis and GUM evaluation results

Based on the experimental data and using Equation (8), the degrees of freedom for the linear fitting were set to 10, while those for the defocus error determination experiment were 14. Applying the Welch–Satterthwaite equation, the effective degrees of freedom were calculated to be 5.83, yielding a coverage factor t_v=2.5. Taking the nominal focal length as 80 mm, the relative uncertainty of the focal length f was determined to be 0.000263.

4 Model construction and evaluation based on MCM

4.1 MCM model considering error propagation

The Monte Carlo Method (MCM) for uncertainty evaluation involves constructing a mathematical model that describes the relationship between the measured quantity and various input variables along with their associated uncertainties. By repeatedly sampling these input variables randomly, a large number of simulated data points are generated to estimate the distribution of the output variable.

However, it is observed that in focal length measurement, there is no direct measurement model available, and the errors do not directly affect the measurement of the relative focal length. Instead, these errors propagate through the measurement of ring diameters and indirectly influence the final result. Specifically, defocus errors and temperature-induced pixel pitch variations contribute to errors in ring diameter measurements, which in turn affect the relative focal length.

Based on this analysis, the simulation model for MCM is still founded on Equation (3), but during computation, random compensation of errors is introduced to simulate the influence of defocus and temperature variations on the focal length. To more accurately evaluate uncertainty, a quadratic fitting method is employed, enabling further refinement of the fitting errors in both the slope and intercept of the corrected model.

Ultimately, the corrected model is simulated using the Monte Carlo method to perform uncertainty evaluation under conditions where error propagation is present, thus achieving uncertainty estimation that accounts for indirect error influences.

4.2 Simulation and results of the MCM method

The uncertainty simulation of the MCM model was performed using MATLAB software. The first step is to determine the number of Monte Carlo sampling iterations M. This was achieved using the a priori experimental method [15], where the value of M is determined according to the following equation:

$$M > 10^4 / p \tag{23}$$

With a confidence level of 95%, p=0.05, the required sample size for Monte Carlo simulation was determined to be: M=10^6.

In this analysis, the defocus error is assumed to follow a uniform distribution, while both the fitting error and the pixel pitch error are assumed to follow a normal distribution.

Prior to performing the curve fitting, the Monte Carlo Method (MCM) is applied to sample these errors. Specifically, compensation is applied to the diameters of the same 12 interference rings (corresponding to i=0~11). After the fitting process, the slope and the subsequently calculated focal length are further compensated based on the sampled errors.

The input parameters used for this MCM simulation are listed in Table 2.

Tab.2 probability distribution of MCM input variables

Input Quantity	Distribution Parameters			
	μ	σ	a	b
Defocus Error, $U_{f_{ad}}$/mm			-0.00795	0.00795
Fitting Error	Obtained from GUM Fitting	0		

With a nominal focal length of 80 mm and a nominal pixel pitch of 0.0028 mm, the uncertainty evaluation results obtained using the Monte Carlo Method (MCM) are summarized in Table 3.

Tab.3 MCM measurement uncertainty results

Evaluation Parameters	Evaluation Results
Average Focal Length,$\bar{f}$/mm	78.36
Relative Focal Length Uncertainty, U_{f_w}/−	0.0000621
Expanded Relative Uncertainty of Relative Focal Length,$U_{r(f_w)}$/−	0.000126
Left Endpoint of the 95% Confidence Interval, D_{Left}/−	19788.73
Right Endpoint of the 95% Confidence Interval,D_{right}/−	19791.76

5 Results analysis

The comparison results show that both the GUM model and the MCM model can obtain the same relative focal length values, but there is a significant difference in the relative expanded uncertainty. To verify the validity of the assessment results, a comparative validation analysis is conducted on the results obtained by the two methods. Through formulas (24) and (25), if the formulas hold true, it can be concluded that the GUM method has passed the validation.

$$d_{\text{low}} = \left|\overline{\alpha} - U_p - y_{\text{low}}\right| \le \delta \tag{24}$$

$$d_{\text{high}} = \left|\overline{\alpha} + U_p - y_{\text{high}}\right| \le \delta \tag{25}$$

where y_{high}、y_{low} are the upper and lower limits of the interval for the confidence probability p obtained by MCM, respectively, while a-U_{p}、a+U_{p} are the upper and lower limits of the interval for the confidence probability p obtained by GUM. From the GUM data, the left endpoint of the 95% confidence interval is 19,790.254277, the right endpoint is 19,790.254352. δ is the tolerance, obtained from Equation (13):

$$\delta = 0.5 \times 10^{m} \tag{26}$$

where m is determined by the number of significant digits of the standard uncertainty [16], so the tolerance is 0.0000005. The calculations show that the absolute values of both d_{low} and d_{high} are greater than the tolerance, indicating that the GUM has not passed the validation by the MCM. To further analyze the reasons, the GUM model and the measurement methods are examined.

5.1 Applicability analysis of the GUM method

When using the GUM method for relative focal length fitting measurement, it is not possible to correct the ring diameter. Therefore, in the final uncertainty synthesis, the uncertainty caused by thermal drift error and the uncertainty brought by defocusing error are considered separately. Thus, the measurement method of the GUM model has an impact on the final expanded relative.

5.2 Distribution characteristic test of relative focal length

There are fundamental differences between the two models in the calculation of relative expanded uncertainty. The MCM generates a large number of random samples and simulates the distribution of measurement results to obtain the expanded uncertainty based on the distribution function. The GUM mainly calculates the expanded uncertainty by assuming the distribution of the measured. In this experiment, the GUM uses the t-distribution for the estimation of relative focal length. The Quantile-Quantile(Q-Q) Plot Method is used to show the comparison between the Monte Carlo simulation results and the t-distribution, which helps to analyze their distribution differences. The results are shown in Figure 7.

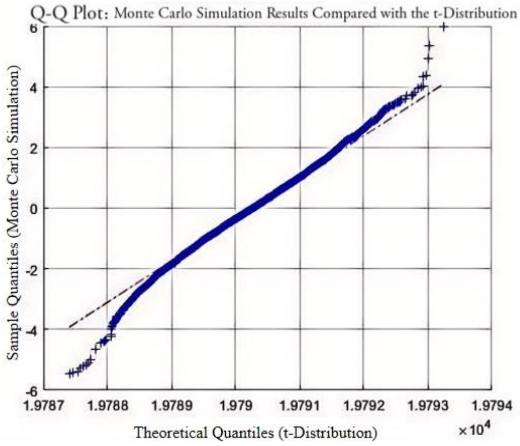

Fig.7 Comparison chart of MCM and t-distribution results

As can be seen from Figure 7, the distribution of the measured mostly conforms to the *t*-distribution, but there are obvious deviations at the ends of the data. Therefore, it can be concluded that the GUM assessment method will cause deviations in the expanded uncertainty, which in turn leads to differences between the two results.

6 Conclusion

Based on a self-calibration measurement method for focal length using a F-P etalon, this study investigates the evaluation results of the same measure and using both the GUM and Monte Carlo (MCM) uncertainty models. Additionally, an evaluation procedure for conducting MCM uncertainty assessment under error propagation conditions is proposed. The measurement uncertainty of the lens focal length measurement system based on the F-P etalon is evaluated using both methods. The results reveal that there is a difference in the expanded relative uncertainty obtained by the two methods. Validation of the GUM approach using the MCM results shows that, within the specified tolerance range, the GUM method fails to pass the validation. Therefore, the MCM method should be adopted for uncertainty evaluation in this scenario. A Q-Q plot is used to test the distribution of the measured relative focal length, and the results indicate that the deviation of the relative focal length distribution from a *t*-distribution is the main reason for the inconsistency in the measurement uncertainty results between the two evaluation methods. The analysis shows that, for a nominal lens focal length of 80 mm, the relative expanded uncertainty is 0.0126%.

This work was funded by National Natural Science Fo undation of China [Grant No.52475577,51875543].

References

[1] Z. Du, W. Wang, Y. Wang et al., High-precision measurement method of laser differential confocal length based on eccentricity suppression. Chinese Journal of Scientific Instrument. **44**, 39-46 (2023).

[2] X. Li,Focal length measurement for thin convex lens based on parallel tube method. Journal of Applied Optics. **40**, 859-862 (2019).

[3] X. Fei, C. Chen, W. Wang et al., Design of lens group focal length measurement system based on object-image parallax comparison. Physical Experiment of College. **33**, 21-24 (2020).

[4] X. He, J. Dou, Y. Hu et al., Focal length measurement based on the correlation coefficient matching strategy. Opt. Laser Eng. 108446 (2024).

[5] X. Cao, Y. Huang, Q. Nguyen et al., Measurement of focal length based on laser-beam-spot tracking system using diffractive beam sampler. Measurement **122**, 135-140 (2018).

[6] J. Dou, X. He, Y. Hu et al., Focal length measurement based on vortex beam interference. Optics and Lasers in Engineering. **178**, 108197 (2024).

[7] M. Yan, W. Gao, S. Zhao et al., Uncertainty evaluation of measurement model of pressure sensor based on Monte Carlo method. Acta Metrologica Sinica. 1-8 (2025).

[8] T. Widmaier, B. Hemming, J. Juhanko et al., Application of Monte Carlo simulation for estimation of uncertainty of four-point roundness measurements of rolls. Precision Engineering. **48**, 181-190 (2017).

[9] M. Wei, Comparative analysis of measurement uncertainty evaluation with Monte Carlo method and GUM. Journal of Electronic Measurement and Instrumentation. **32**(11), 17-25 (2018).

[10] X. Shen, Z. Sun, J. Hu et al., Method for measuring focal length of transmission objective lens based on F-P etalon. Chinese Journal of Science Instrument. **39**(5), 1-8 (2018).

[11] Q. Chen, J. Yan, Z. Liu et al., An air refractometer with dual vacuum chambers based on the method of equivalent synthetic wave. Acta Metrologica Sinica. **25**(3), 203-206 (2004).

[12] S. Liu, Y. Chang, Z. Xiao et al., Accurate calculation of the spacing of F-P etalon under the multi-wavelength weighted regression. Infrared and Laser Engineering. **40**(3), 529-532 (2011).

[13] X. Lan, Micro angel measurement method and experimental research based on F-P etalon. Master's thesis, China Jiliang University (2020).

[14] H. Zhu, Z. Xiao, Y. Hou et al., A method for measuring focal length and rotation angle using Fabry-Perot etalon. China Patent CN201510217472.7, September 20, 2019.

[15] M. Song, W. Wang, Determination of simulation sample size M in measurement uncertainty evaluation using Monte Carlo method. Acta Metrologica Sinica. **31**(1), 91-96 (2010).

[16] L. Li, X. Shen, X. Zhang et al., Uncertainty analysis and experimental study of Micro-angel measuring device. Research and Exploration in Laboratory. **43**(6), 1-6+15 (2024).